Fig. S1

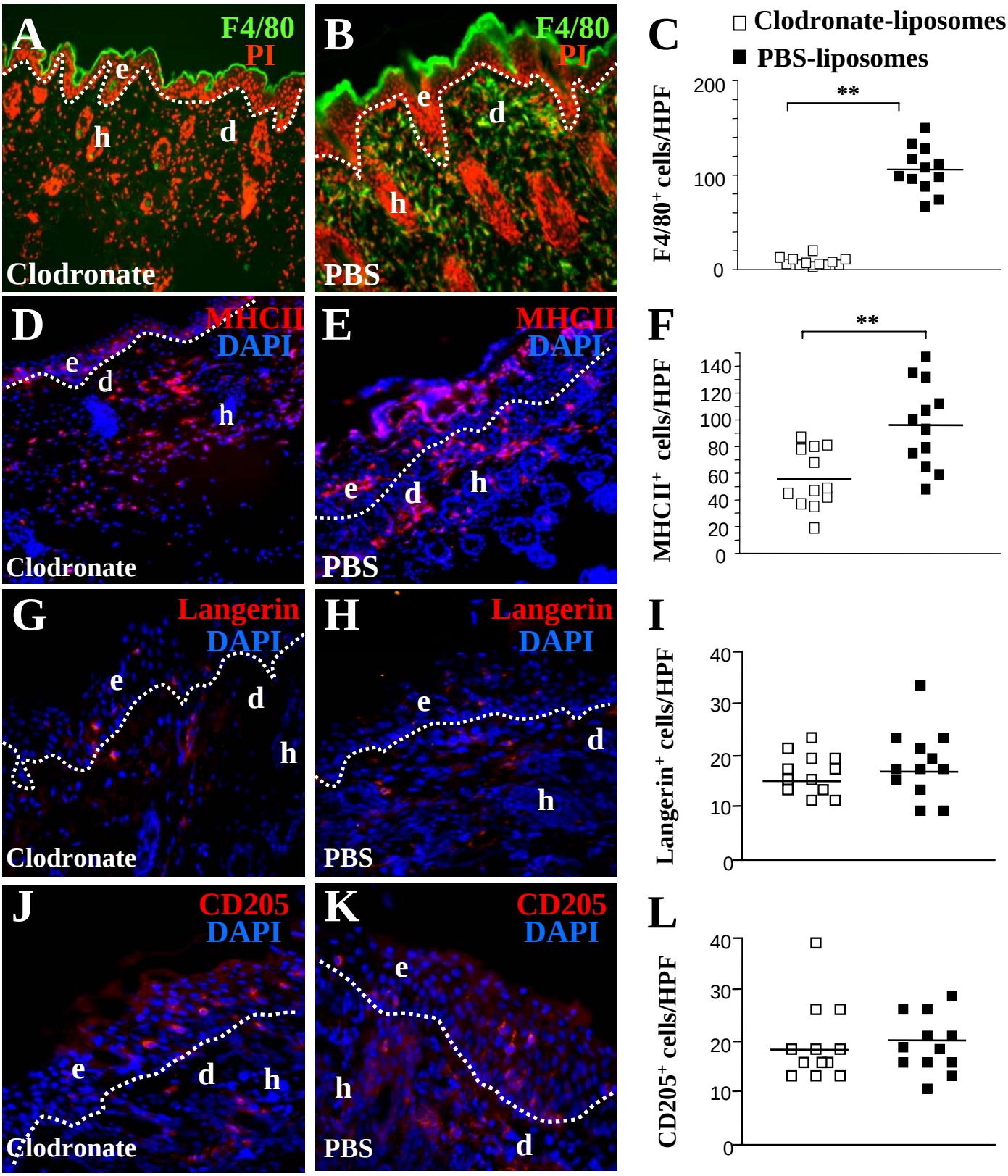
A
F4/80
PI
e
h
d
Clodronate
B
F4/80
PI
e
d
h
PBS
C
Clodronate-liposomes
PBS-liposomes
**
F4/80+ cells/HPF
200
100
0
D
MHCII
DAPI
e
d
h
Clodronate
E
MHCII
DAPI
e
d
h
PBS
F
**
MHCII+ cells/HPF
140
120
100
80
60
40
20
0
G
Langerin
DAPI
e
d
h
Clodronate
H
Langerin
DAPI
e
d
h
PBS
I
Langerin+ cells/HPF
40
30
20
10
0
J
CD205
DAPI
e
d
h
Clodronate
K
CD205
DAPI
e
h
d
PBS
L
CD205+ cells/HPF
40
30
20
10
0

Fig. S1

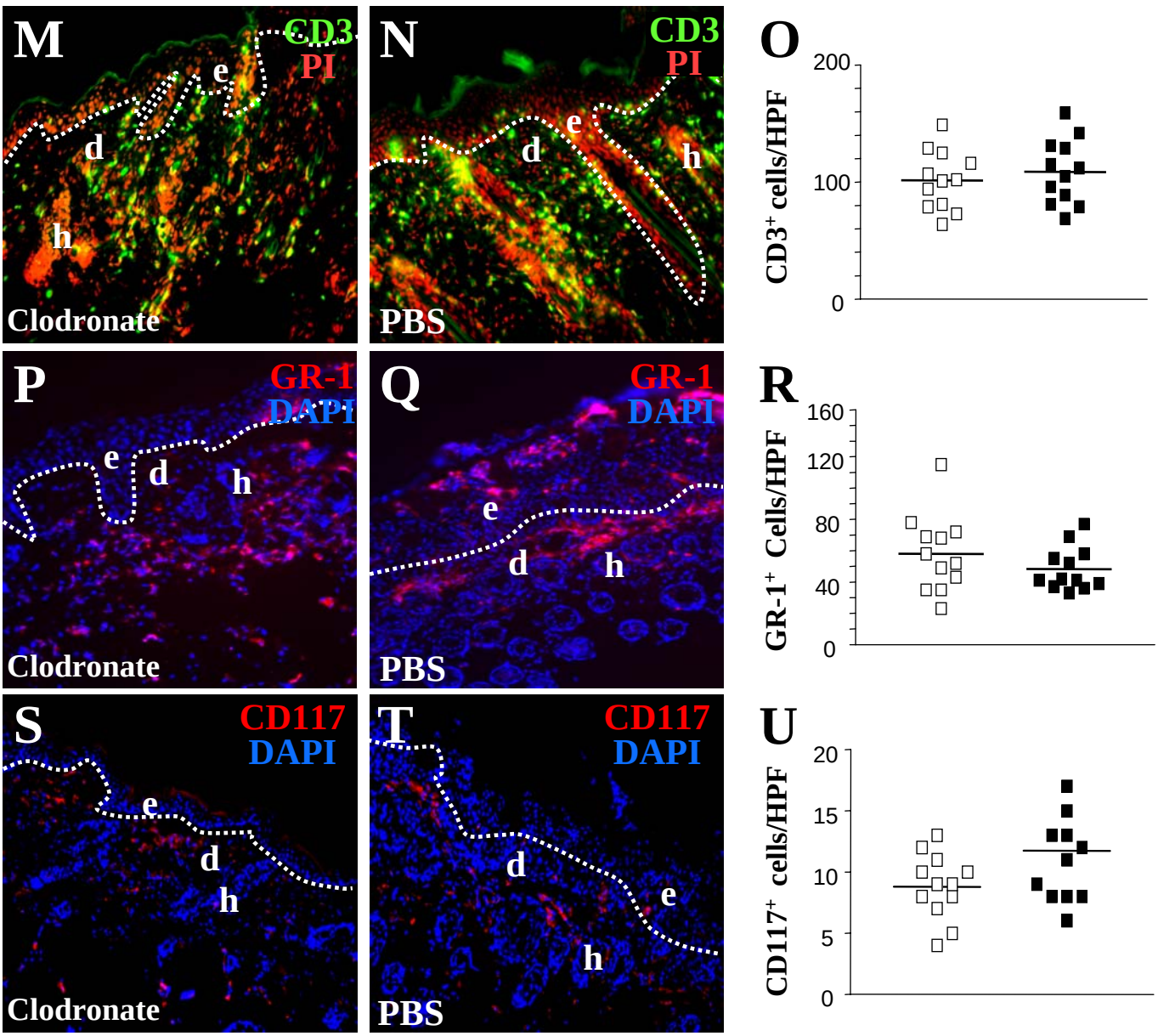
M
CD3
PI
e
d
h
Clodronate
N
CD3
PI
e
d
h
PBS
O
200
100
0
CD3+ cells/HPF
P
GR-1
DAPI
e
d
h
Clodronate
Q
GR-1
DAPI
e
d
h
PBS
R
160
120
80
40
0
GR-1+ Cells/HPF
S
CD117
DAPI
e
d
h
Clodronate
T
CD117
DAPI
d
e
h
PBS
U
20
15
10
5
0
CD117+ cells/HPF

Fig. S2

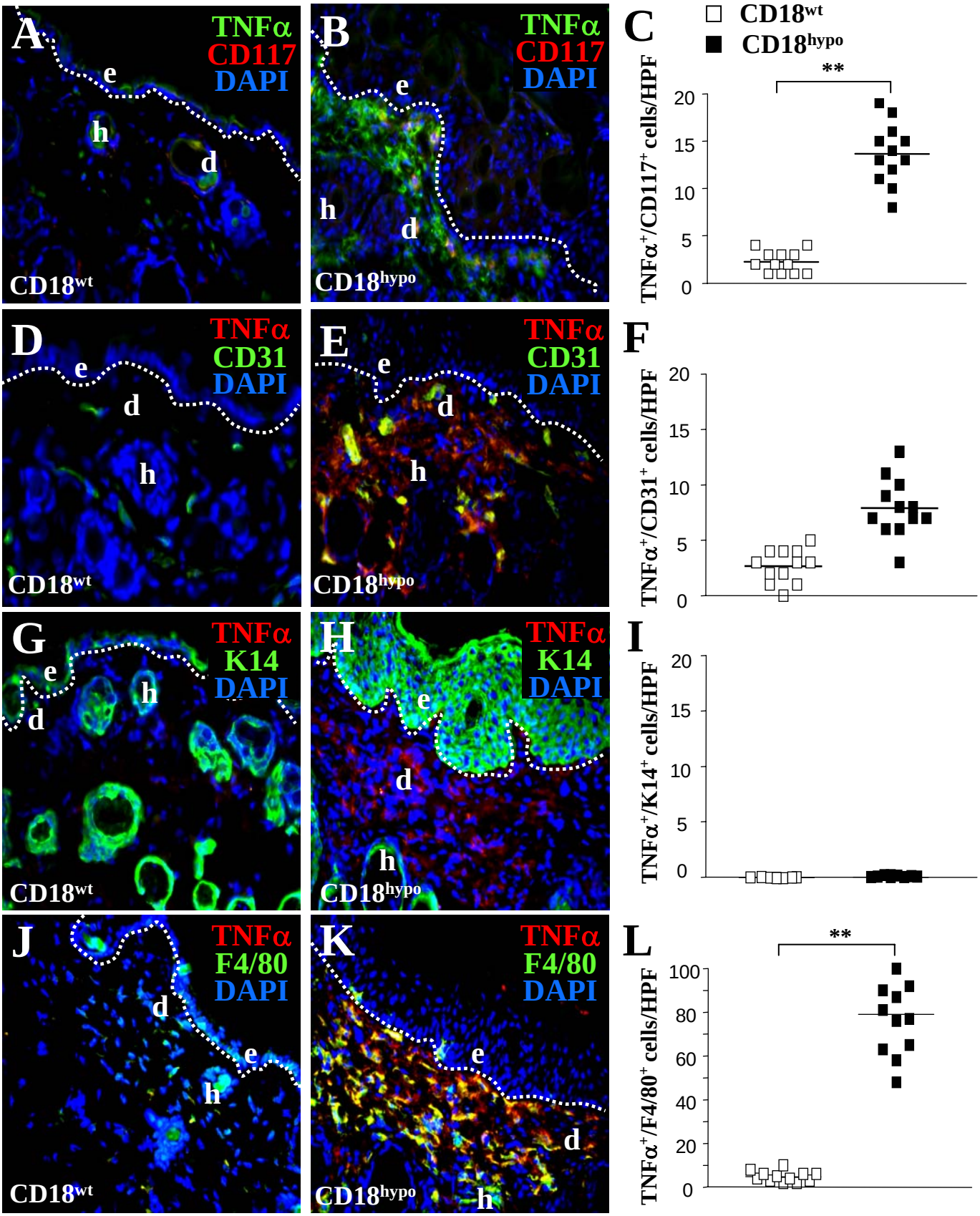
A
TNFα
CD117
DAPI
e
h
d
CD18wt
B
TNFα
CD117
DAPI
e
h
d
CD18hypo
C
CD18wt
CD18hypo
**
TNFα+/CD117+ cells/HPF
20
15
10
5
0
D
TNFα
CD31
DAPI
e
d
h
CD18wt
E
TNFα
CD31
DAPI
e
d
h
CD18hypo
F
TNFα+/CD31+ cells/HPF
20
15
10
5
0
G
TNFα
K14
DAPI
e
h
d
CD18wt
H
TNFα
K14
DAPI
e
d
h
CD18hypo
I
TNFα+/K14+ cells/HPF
20
15
10
5
0
J
TNFα
F4/80
DAPI
d
e
h
CD18wt
K
TNFα
F4/80
DAPI
e
d
h
CD18hypo
L
**
TNFα+/F4/80+ cells/HPF
100
80
60
40
20
0

Fig. S3

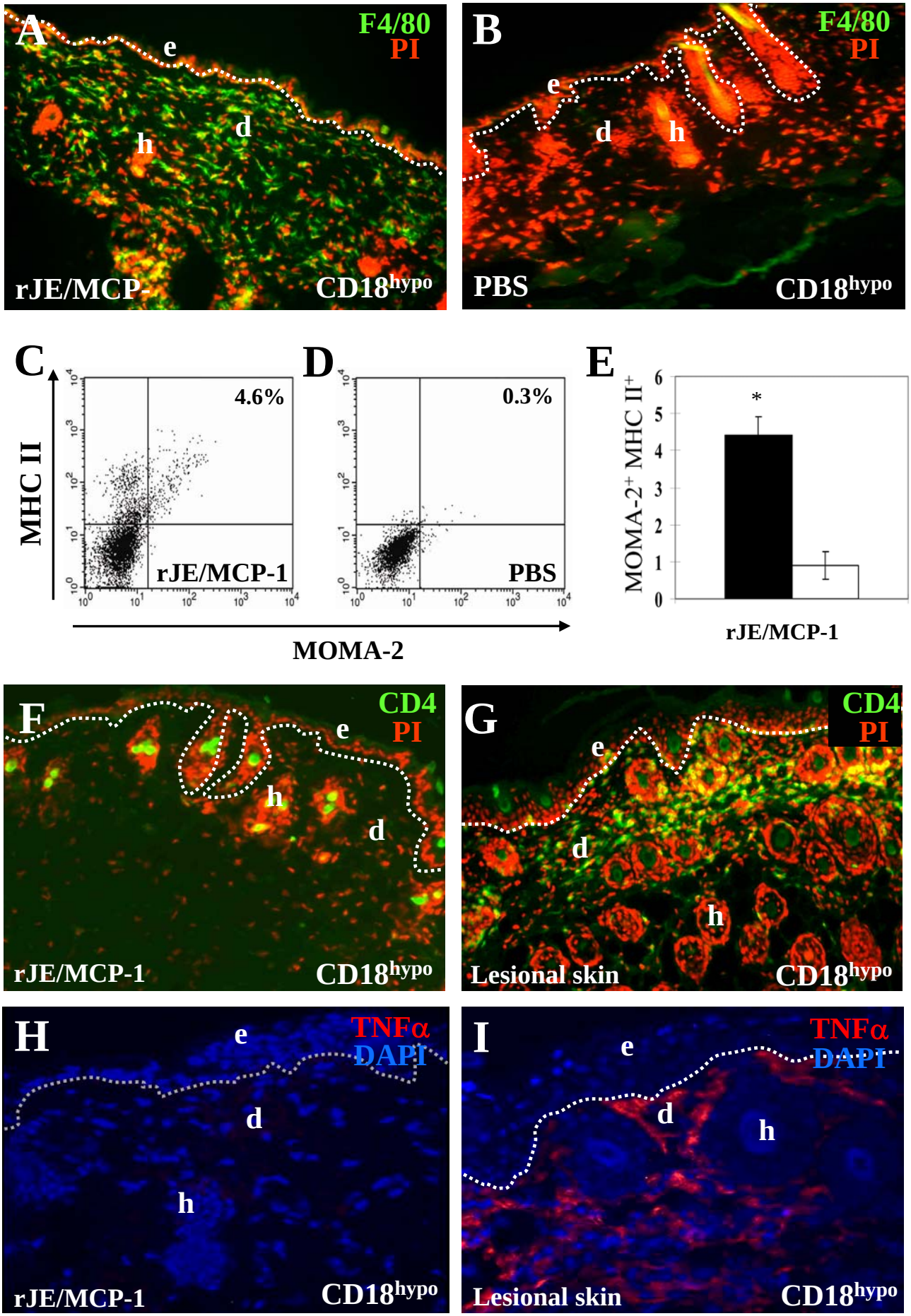
A
F4/80
PI
e
h
d
rJE/MCP-
CD18hypo
B
F4/80
PI
e
d
h
PBS
CD18hypo
C
MHC II
4.6%
rJE/MCP-1
D
0.3%
PBS
MOMA-2
E
MOMA-2+ MHC II+
*
rJE/MCP-1
F
CD4
PI
e
h
d
rJE/MCP-1
CD18hypo
G
CD4
PI
e
d
h
Lesional skin
CD18hypo
H
TNFα
DAPI
e
d
h
rJE/MCP-1
CD18hypo
I
TNFα
DAPI
e
d
h
Lesional skin
CD18hypo

Fig. S4

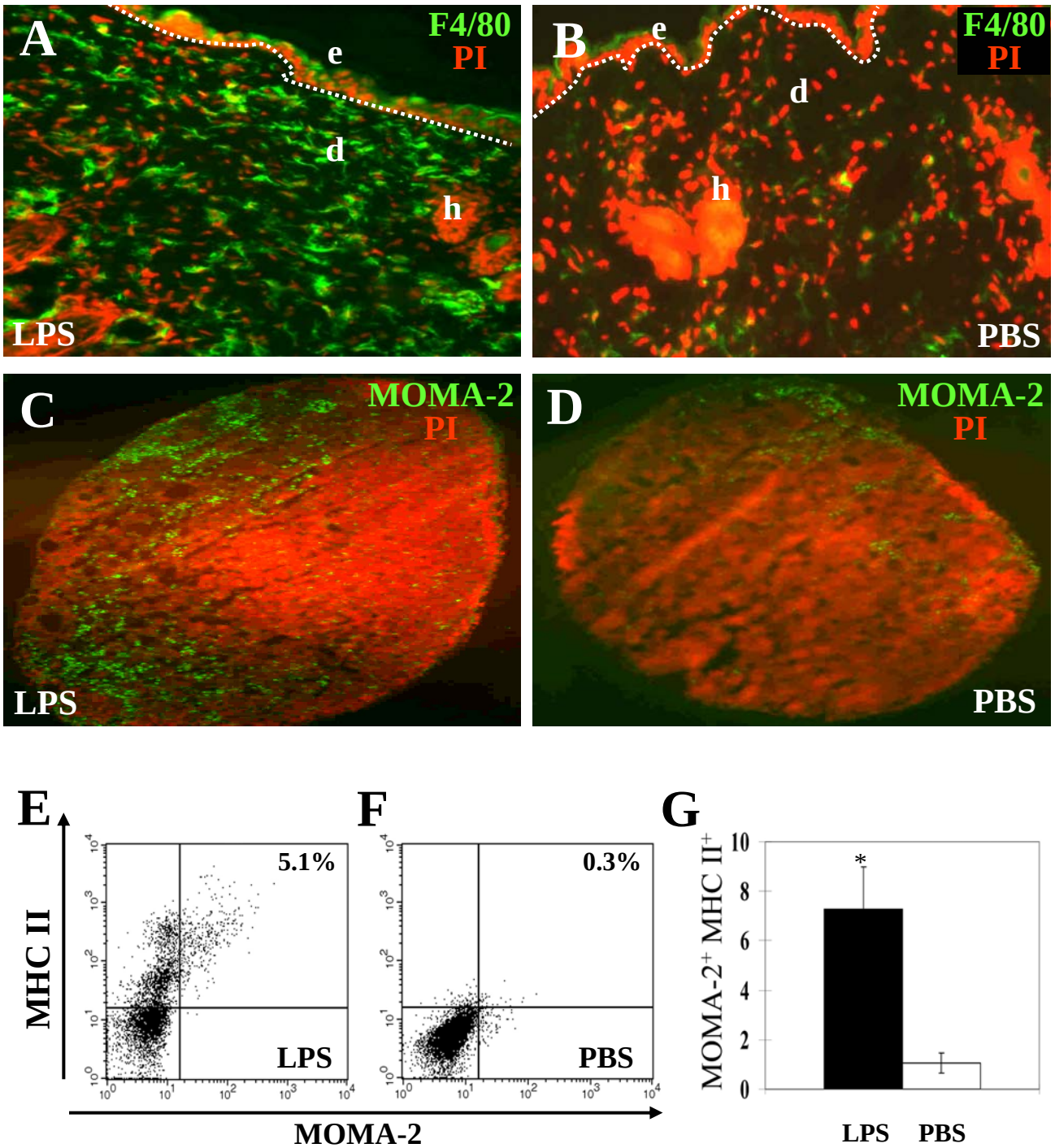
A
F4/80
PI
e
d
h
LPS
B
e
F4/80
PI
d
h
PBS
C
MOMA-2
PI
LPS
D
MOMA-2
PI
PBS
E
MHC II
5.1%
LPS
MOMA-2
F
0.3%
PBS
G
MOMA-2+ MHC II+
10
8
6
4
2
0
*
LPS
PBS

Fig. S4

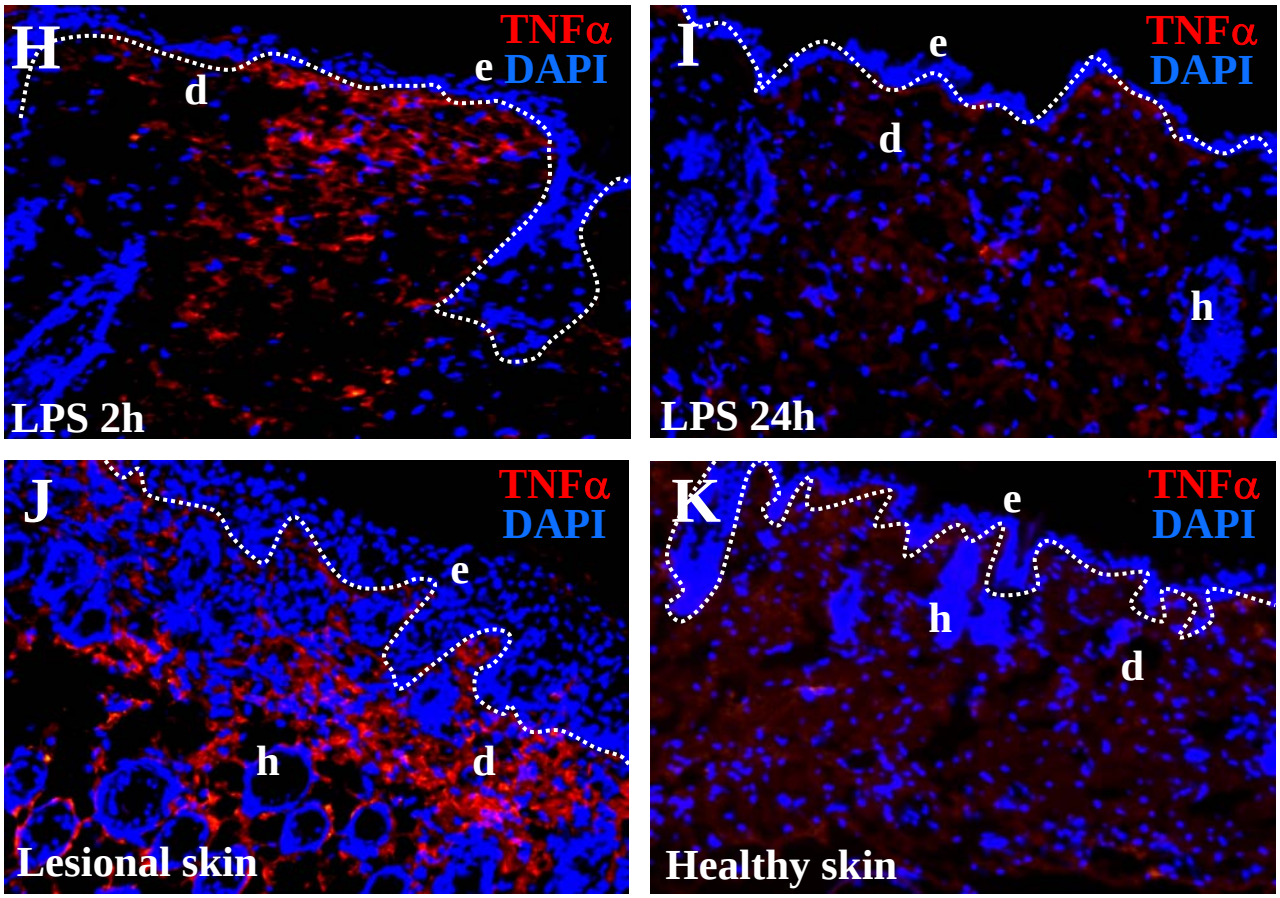
H
TNFα
DAPI
e
d
LPS 2h
I
TNFα
DAPI
e
d
h
LPS 24h
J
TNFα
DAPI
e
h
d
Lesional skin
K
TNFα
DAPI
e
h
d
Healthy skin

Fig. S5

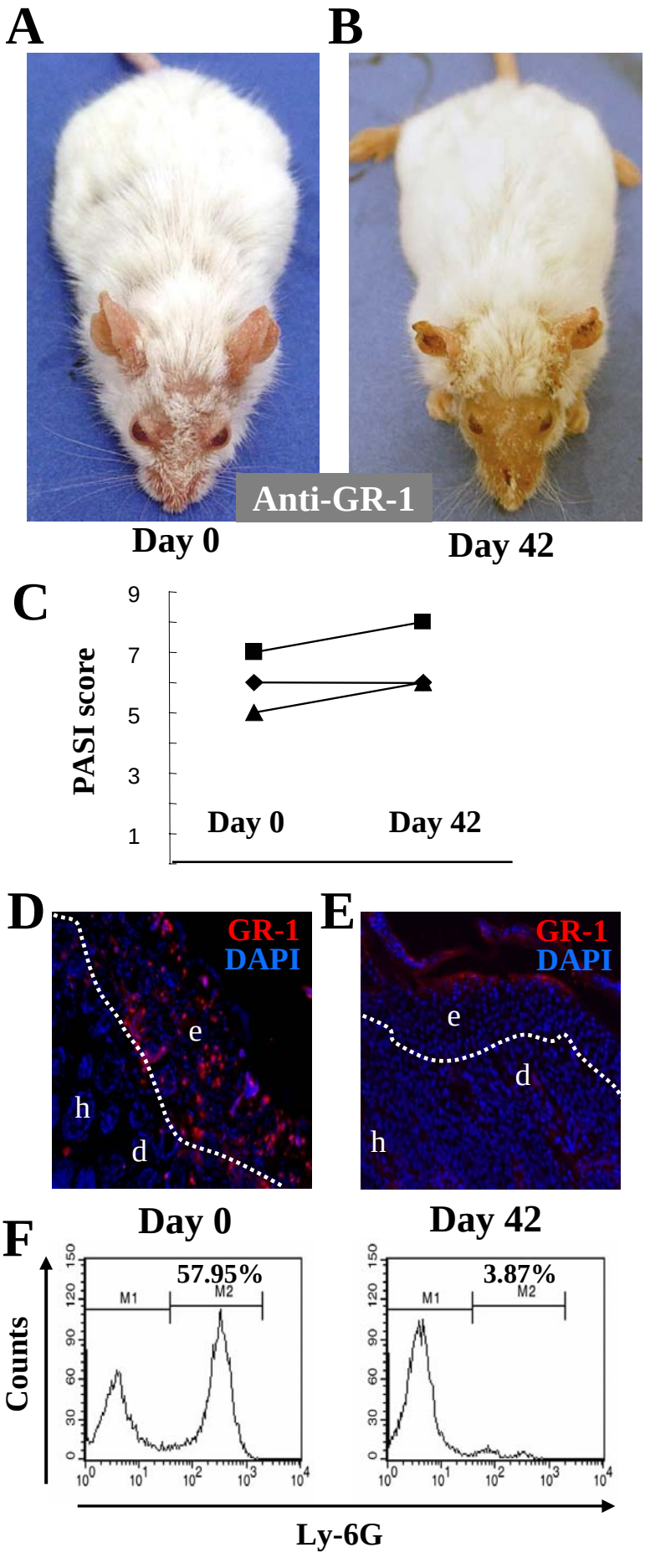
A
B
Anti-GR-1
Day 0
Day 42
C
PASI score
9
7
5
3
1
Day 0
Day 42
D
GR-1
DAPI
e
h
d
E
GR-1
DAPI
e
d
h
F
Day 0
Day 42
57.95%
3.87%
M1
M2
Counts
Ly-6G

Supplementary information to the manuscript by Wang *et al.*

"Activated Macrophages are Essential in a Murine Model for T Cell-Mediated Chronic Psoriasiform Skin Inflammation"

SUPPLEMENTARY RESULTS

Treatment with liposome-encapsulated clodronate results in selective depletion of macrophages

The specificity of clodronate liposomes for the depletion of phagocytic cells has repeatedly been shown (37-39, 59, 62). We furthermore found that clodronate liposomes specifically depleted macrophages from the skin 24 h after injection (Figure S1 A,B,C). As MHC II expression occurs on macrophages as well as on dendritic cells and Langerhans cells, it is expected that the fraction of MHC II positive macrophages is depleted after clodronate treatment (Figure S1 D,E,F). Langerin specifically detects Langerhans cells. Langerin$^+$ cell counts were the same in the clodronate-injected mice compared to the PBS injected controls (Figure S1 G,H,I). CD11c would be a distinct marker to differentiate macrophages from dendritic cells. Given the fact that we are studying a CD18 hypomorphic mutant with a decrease in CD18 expression to 2-16% of wild type, the CD11c molecules will also be reduced to a level where immunostaining has been proven to be unreliable. Therefore, we have used an antibody directed against CD205, a marker expressed by both dendritic cells and Langerhans cells in the skin (63). There was no decrease in CD205$^+$ cells in clodronate treated mice compared to PBS

treated controls (Figure S1 J,K,L). Also a small population of dermal cells staining positive for the dendritic cell specific marker CD83 was identical in clodronate injected $CD18^{hypo}$ compared to PBS injected $CD18^{hypo}$ mice (data not shown). Furthermore, clodronate had no significant effect on T cells (Figure S1 M,N,O), neutrophils (Figure S1 P,Q,R) or mast cells (Figure S1 S,T,U). However, after clodronate-induced macrophage depletion, Stratis et al. (see this issue) observed a reduction in numbers of $GR\text{-}1^{+}$ neutrophils 3 to 4 days after initiation of clodronate treatment, while in the $CD18^{hypo}$ PL/J mouse model no reduction in neutrophil counts occurred after clodronate injection, at least not within the first 24 hours. At this early time-point, only macrophages were efficiently depleted in the chronically diseased skin of $CD18^{hypo}$ mice. Nevertheless, histological characteristics of a severe psoriasiform inflammation, such as hyperkeratosis, presence of T cells and also of neutrophils (including micro-abscesses), persisted 24 hours after clodronate injection, despite the rapid elimination of macrophages. Similar to human psoriasis, or other states of chronic skin inflammation in humans, substantial reversal of the chronic skin disease needs days to several weeks in $CD18^{hypo}$ mice. Once inflammation is repressed in $CD18^{hypo}$ PL/J mice, no neutrophils could be detected in the healed skin, which was the case at 4 to 6 weeks after treatment with clodronate liposomes. Such a removal of neutrophils from inflamed skin of mice may proceed more rapidly in the model of IKK2 deficiency as presented by Haase et al. in this issue, since in that case, mice suffer from a disease of high acuity rather than from a chronic inflammation.

Although neutrophils may, due to their phagocytic activity, also to some extent be depleted by clodronate liposomes, this proportion is hard to quantify, since neutrophils

are rapidly replenished and substituted by other infiltrating neutrophils from the blood stream. This may have also hampered our measurement of potentially clodronate-depleted neutrophils in CD18^{hypo} skin.

In addition to macrophages, infiltrating mast cells and endothelial cells are additional sources of TNF-α in the lesional skin of CD18^{hypo} PL/J mice

While in CD18 wild type mice almost no mast cells stained for TNF-α, the number of TNF-α-containing mast cells significantly increased in lesional skin of CD18^{hypo} mice (Figure S2 A,B,C). In addition, endothelial cells did not stain for TNF-α in CD18 wild type mice, while there was distinct double staining for endothelial cells (CD31) and TNF-α in lesional skin of CD18^{hypo} mice (Figure S2 D,E,F). Neither in keratinocytes of CD18 wild type mice nor in the lesional skin of CD18^{hypo} mice was TNF-α produced (Figure S2 G,H,I). In contrast, macrophages represented an important source of TNF-α-producing cells in the lesional skin of CD18^{hypo} PL/J mice, but not in wild type mice (Figure S2 J,K,L).

Administration of murine recombinant JE/MCP-1 recruits macrophages to the skin of healthy CD18^{hypo} mice, but fails to cause psoriasiform inflammatory skin disease

As MCP-1 is an important chemokine for the recruitment of monocytes/macrophages, we were interested whether administration of rJE/MCP-1 would be sufficient to trigger the psoriasiform phenotype in healthy CD18^{hypo} mice. Healthy CD18^{hypo} mice (n =4) were injected i.d. with either 0.2 μg murine rJE/MCP-1 or with PBS as control once a week. Despite a significant accumulation of F4/80^{+} macrophages in the dermis after eight weeks

of administration, rJE/MCP-1 injection failed to trigger the psoriasiform skin disease in these mice. To investigate the macrophage recruiting capacity of rJE/MCP-1, skin sections were stained for macrophage markers before and after injection with rJE/MCP-1 or PBS. Skin sections of rJE/MCP-1-treated mice showed significant accumulation of $F4/80^{+}$ macrophages in the dermis (Figure S3 A), while macrophages were not recruited by PBS injections (Figure S3 B). Similarly, rJE/MCP-1-treated mice showed an increased infiltration of monocytes/macrophages in skin DLNs of healthy $CD18^{hypo}$ mice (Figure S3 C), when compared to PBS-treated control mice (Figure S3 D). This increase in macrophage recruitment was significant ($p < 0.05$) (Figure S3 E). However, macrophages recruited by rJE/MCP-1 were not able to recruit $CD4^{+}$ T cells to the injected skin areas (Figure S3 F). This finding is in contrast to high numbers of $CD4^{+}$ T cells in lesional skin of affected $CD18^{hypo}$ mice (Figure S3 G). We therefore addressed the question whether rJE/MCP-1 recruited macrophages may not have sufficiently been activated to release TNF-α. In fact, as shown by immunofluorescence, TNF-α was not expressed in rJE/MCP-1-injected skin areas (Figure S3 H), whereas a strong immunostaining for TNF-α was observed in lesional skin of affected $CD18^{hypo}$ mice (Figure S3 I).

Administration of LPS recruits and partially activates macrophages in the skin and skin draining lymph nodes, while it fails to cause psoriasiform inflammatory skin disease in healthy $CD18^{hypo}$ mice

Activation of macrophages appears to be required to elicit the psoriasiform inflammatory skin disease in healthy skin of $CD18^{hypo}$ mice. As macrophages were not activated to release proinflammatory cytokines such as TNF-α after rJE/MCP-1 injection, we

employed intradermal injection of bacterial LPS to recruit and possibly activate macrophages in vivo. As TNF-α has been reported to disappear rapidly after LPS injection (42), we administrated intradermally 25 μg LPS into healthy $CD18^{hypo}$ mice once a day or, alternatively, once a week for six weeks. Neither of the LPS injection schedules was sufficient to elicit the psoriasiform inflammatory skin disease even after an observation period of six weeks. Twenty-four hours after LPS injection, we observed an abundant population of macrophages in the LPS injected skin areas (Figure S4 A), compared to PBS treated control mice (Figure S4 B). A similar result was obtained in skin DLNs as assessed by immunofluorescence staining (Figure S4 C, D) or by quantification in FACS analysis of the lymph nodes after treatment with LPS (Figure S4 E) or PBS control (Figure S4 F). This increased macrophage recruitment was significant (p <0.05) (Figure S4 G). To study whether TNF-α is transiently expressed following injection of LPS, immunostaining was performed on cryosections derived from injected skin areas two and 24 hours post-injection of LPS and from lesional skin of affected $CD18^{hypo}$ mice. In fact, TNF-α was detectable in the dermis two hours after LPS treatment (Figure S4 H), but no longer after 24 hours (Figure S4 I). As expected, strong TNF-α expression was found in lesional skin of affected $CD18^{hypo}$ mice (Figure S4 J), but not in healthy skin (Figure S4 K).

Neutrophils do not contribute to the development of the chronic psoriasiform skin inflammation in $CD18^{hypo}$ PL/J mice

Neutrophils are a constant feature in psoriatic lesions of humans, forming the micro-abscesses of Munro, which are also a hallmark in inflammatory skin lesions of $CD18^{hypo}$

PL/J mice. To investigate a potential causal role of neutrophils in the pathogenesis of the psoriasiform inflammatory skin lesions in $CD18^{hypo}$ PL/J mutants, we have depleted neutrophils using neutrophil depleting antibodies such as anti Ly-6c and Ly-6G (GR-1) mAb. FACS analysis confirmed successful depletion of neutrophils in peripheral blood, while immunostaining for GR-1^{+} cells indicated the absence of neutrophils in the skin. Complete depletion of neutrophils in the blood and in the skin even over 6 weeks did not result in significant improvement of the psoriasiform inflammatory skin disease, neither clinically, – as assessed by the adapted PASI score, – nor histologically (Figure S5).

SUPPLEMENTARY SECTION - METHODS

In vivo depletion of macrophages using liposome-encapsulated clodronate

Macrophages were depleted in vivo using dichloromethylene diphosphonate (clodronate) encapsulated liposomes as described earlier in the Methods section of the main manuscript. Liposomes are used as Trojan horse to get the small clodronate molecules into the macrophage. Once ingested by macrophages, the phospholipid bilayers of liposomes are disrupted under the influence of lysosomal phospholipases. The hydrophilic clodronate molecules which are intracellularly released following lysosomal disintegration cannot diffuse out of the cell since they cannot cross cellular membranes. As a result the intracellular clodronate concentration increases as long liposomes are present to be ingested and digested. Defined clodronate concentrations result in irreversible damage and macrophage apoptosis. Importantly, clodronate molecules released in the circulation from dead macrophages cannot enter cells, because they are not able to pass through cell membranes. The combination of low toxicity and short half life makes clodronate a feasible and effective approach for the liposome-mediated elimination of macrophages in vivo (64, 65). Apart from their efficacy, clodronate liposomes deplete macrophages with high selectivity due to the fact that liposomes of more than a few hundred nanometers will not be internalized by non-phagocytic cells, and cells with less avid phagocytosis compared to macrophages, such as dendritic cells. Hence, other cells such as lymphocytes, granulocytes or mast cells are not depleted by multilamellar clodronate liposomes (37). In addition, typical dendritic cells (DC), as localized in the T cell areas in the spleen and lymph nodes will not be depleted by iv administration of clodronate liposomes (62).

Intradermal injection of recombinant JE/MCP-1 and LPS

0.2 μg of mouse rJE/MCP-1 (R&D Systems GmbH) or 25 μg LPS from *E. coli* 011:B4 (InvivoGen) in 200 μl of PBS was injected intradermally at four sites (50 μl/site) on the back of each healthy $CD18^{hypo}$ mouse. As control, 200 μl of PBS was used. Injection of LPS was carried out once a day or once a week in three mice for a total period of six weeks. Seven days after the last injection of rJE/MCP-1 or at two and 24 hours after the last administration of LPS, injected skin areas were excised and subjected to immunostaining. Cells from DLNs derived from both rJE/MCP-1 treated and PBS treated mice were prepared for FACS analysis as described in the Methods section of the main manuscript.

Immunofluorescence staining

For immunofluorescence analysis frozen sections from indicated skin specimens were stained with the indicated antibodies. Where available, antibodies directly conjugated with fluorophores have been used: Alexa®488-conjugated rat anti-mouse F4/80 IgG2b (Caltag Laboratories®, clone: CI:A3-1), Alexa®488-conjugated hamster- anti-mouse CD3 IgG (Caltag Laboratories®, clone: 500A2), PE-conjugated rat-anti-mouse MHC class II IgG2b (Miltenyi Biotec GmbH, clone: M5/114.15.2). Otherwise, purified or biotinylated antibodies were applied as primary antibodies: goat-anti-mouse CD207 (Langerin) polyclonal Ab IgG (Santa Cruz Biotechnology, Inc), rat-anti-mouse TNF-α mAb IgG1 (BD Pharmingen, clone MP6-XT22), rat-anti-mouse CD31 (PECAM-1) mAb IgG2a (BD Pharmingen, clone: MEC 13.3), rat-anti-mouse Ly-6G and Ly-6C (GR-1) mAb IgG2b (BD Pharmingen, clone: RB6-8C5), biotinylated rat-anti-mouse CD117

IgG2b (BD Pharmingen, clone: 3C1), rabbit-anti-mouse Keratin 14 (K14) polyclonal Ab IgG (Covance Inc.); secondary antibodies were fluorophore-coupled goat-anti-rat Alexa®488, goat-anti-rat Cy3, goat-anti-rabbit Alexa®488, goat-anti-rabbit Cy3 or streptavidin-Cy3 (all from Caltag Laboratories®). The specificity of the staining was confirmed using appropriate isotype controls: Alexa®488- or Alexa®555-conjugated rat IgG1, rat IgG2a, rat IgG2b, rabbit IgG, hamster IgG and goat IgG. Pictures were taken using a fluorescence microscope Zeiss Axiophot 2 plus e (Carl Zeiss Inc.), with a digital color camera and corresponding software (Axiocam®, Zeiss). All images were processed for printing using Adobe Photoshop® software.

In vivo depletion of neutrophils

Neutrophils were depleted in vivo using anti-mouse Ly-6G and Ly-6C (GR-1) mAb (BD Biosciences). Severely affected $CD18^{hypo}$ PL/J mice were treated with 250 μg anti GR-1 mAb or isotype control antibodies which served as negative control. GR-1 antibodies or isotype control antibodies were injected intraperitoneally twice a week for 6 weeks. Neutrophil depletion was confirmed by FACS analysis from peripheral blood and by immunofluorescence staining against $GR\text{-}1^{+}$ cells in skin specimens. Before and after treatment, disease severity was determined using an adapted psoriasis activity and severity index (PASI) as previously described (21).

SUPPLEMENTARY SECTION – REFERENCES

62. Leenen, P.J., Radosevic, K., Voerman, J.S., Salomon, B., van Rooijen, N., Klatzmann, D., and van Ewijk, W. 1998. Heterogeneity of mouse spleen dendritic cells: in vivo phagocytic activity, expression of macrophage markers, and subpopulation turnover. *J Immunol* 160:2166-2173.

63. Kraal, G., Breel, M., Janse, M., and Bruin, G. 1986. Langerhans' cells, veiled cells, and interdigitating cells in the mouse recognized by a monoclonal antibody. *J Exp Med* 163:981-997.

64. Claassen, I., Van Rooijen, N., and Claassen, E. 1990. A new method for removal of mononuclear phagocytes from heterogeneous cell populations in vitro, using the liposome-mediated macrophage 'suicide' technique. *J Immunol Methods* 134:153-161.

65. van Rooijen, N., Bakker, J., and Sanders, A. 1997. Transient suppression of macrophage functions by liposome-encapsulated drugs. *Trends Biotechnol* 15:178-185.

SUPPLEMENTARY SECTION - FIGURE LEGENDS

Figure S1: Selective depletion of macrophages in the skin following subcutaneous administration of clodronate liposomes. Clodronate liposomes or control PBS liposomes were injected subcutaneously at a dose of 200 µl in affected $CD18^{hypo}$ mice. Skin samples taken 24 hours after liposome administration were examined for qualitative and quantitative characterization of the inflammatory infiltrate. Cryosections derived from affected $CD18^{hypo}$ mice treated with clodronate liposomes or PBS liposomes were stained with anti-mouse F4/80-Alexa®488 for infiltrating macrophages (green) (**A, B**), anti-mouse I-A^b-PE (MHCII) for antigen presenting macrophages, dendritic cells and Langerhans cells (red) (**D, E**) anti-mouse CD207-Cy3 (Langerin) for Langerhans cells (red) (**G**, **H**), anti-mouse CD205-Cy3 for Langerhans/dendritic cells (red) (**J**, **K**), anti-mouse CD3-FITC for T cells (green) (**M, N**), anti-mouse GR-1-PE for granulocytes (red) (**P, Q**), and with CD117-Cy3 for mast cells (red) (**S, T**). Cell nuclei were counterstained with DAPI (blue) or PI (red) (original magnification, ×20). e, epidermis; d, dermis; h, hair follicle. Dotted lines indicate the border between epidermis and dermis. Quantitative analysis and comparison of the infiltrate was performed by counting lesional positively stained cells for F4/80 (**C**), MHCII (**F**), Langerin (**I**), CD205 (**L**), CD3 (**O**), GR-1 (**R**), and CD117 (**U**) in clodronate liposomes treated- compared to PBS-treated lesional skin of $CD18^{hypo}$ mice. Data are presented as median of positive counts in 12 high power fields (HPF) (x40) (n = 12); ** $p < 0.01$ by Student's t test.

Figure S2: In addition to high numbers of TNF-α-containing macrophages, mast cells and endothelial cells are sources of TNF-α in the lesional skin of $CD18^{hypo}$ PL/J mice. To investigate the cellular origin of TNF-α in lesional skin infiltrate, skin samples from $CD18^{wt}$ and affected $CD18^{hypo}$ mice were double stained with anti-mouse TNF-α-FITC (green) or TNF-α-PE (red) together with the cell specific markers CD117-Cy3 anti-mouse for mast cells (red) (**A, B**), CD31-Alexa®488 for endothelial cells (green) (**D, E**), K14-Alexa®488 for keratinocytes (green) (**G, H**) and F4/80-Alexa®488 for macrophages (green) (**J, K**). The overlay (yellow) represents TNF-α producing cells. Cell nuclei were counterstained with DAPI (blue) (original magnification, ×20). e, epidermis; d, dermis; h, hair follicle. Dotted lines indicate the border between epidermis and dermis. Quantitative analysis of the TNF-α producing cells was performed by counting the cells staining positively for both TNF-α and one of the cell markers CD117-Cy3 for mast cells (**C**), CD31 for endothelial cells (**F**), K14 for keratinocytes (**I**) and F4/80 for macrophages (**L**) (yellow dots) in the lesional skin of $CD18^{hypo}$ mice compared to $CD18^{wt}$ mice. Data are presented as median of positive counts in 12 high power fields ($n = 12$); ** $p < 0.01$ by Student's *t* test.

Figure S3: Local injection of rJE/MCP-1 does not result in the psoriasiform skin inflammatory phenotype in $CD18^{hypo}$ mice. To investigate the clinical effect of rJE/MCP-1 treatment, either rJE/MCP-1 or PBS as control were injected intradermally at a dose of 0.2 μg/mouse weekly. rJE/MCP-1 failed to induce psoriasiform skin inflammation in healthy skin of $CD18^{hypo}$ PL/J mice. rJE/MCP-1 or PBS treatment was assessed for macrophage recruitment and activation by immunostaining cryosections from injected

skin areas. rJE/MCP-1-treated mice showed significant accumulation of $F4/80^+$ macrophages in the dermis (**A**) while macrophages were not recruited by PBS injections (**B**). (macrophages, green; cell nuclei, red (propidium iodide PI); original magnification, x20). Similar results were observed in skin DLNs as shown by FACS analysis, where $MOMA\text{-}2^+MHCII^+$ macrophages were increased in healthy $CD18^{hypo}$ mice injected with the rJE/MCP-1 (**C**) compared to controls treated with PBS (**D**). * $p < 0.05$ (**E**). To investigate the recruitment of $CD4^+$ T cells, rJE/MCP-1 injected skin and lesional skin of affected $CD18^{hypo}$ mice were subjected to immunofluorescence staining with FITC-conjugated rat anti-mouse CD4 (green) and propidium iodide for nuclei (red). rJE/MCP-1 injection was not able to recruit $CD4^+$ T cells to injected skin areas (**F**) compared to many $CD4^+$ T cells in skin of affected $CD18^{hypo}$ mice (**G**) (original magnification, x20). TNF-α expression by infiltrating cells was assessed by staining with anti-mouse TNF-α mAb (red) and DAPI for nuclei (blue). TNF-α was absent in rJE/MCP-1-injected skin areas (**H**), whereas a strong immunostaining for TNF-α was observed in lesional skin of affected $CD18^{hypo}$ mice (**I**). (original magnification, x40). One representative experiment out of $n \geq 3$ is shown. e, epidermis, d, dermis, h, hair follicle. Dotted lines indicate the border between epidermis and dermis.

Figure S4: Local LPS administration did not induce the psoriasiform skin inflammation in healthy $CD18^{hypo}$ mice. 25 μg LPS in 200 μl or PBS as control were injected intradermally at four sites (50 μl/site) on the back of healthy skin of $CD18^{hypo}$ mice once a day ($n = 3$) or once a week for six weeks ($n = 3$). At two or 24 hours after the last injection, the injected skin areas and cervical lymph nodes were prepared for immunohistology or

FACS analysis. An abundant population of F4/80^{+} macrophages (green) was observed in the LPS injected skin areas (**A**), compared to PBS treated control mice (**B**). Similar results were obtained for MOMA-2^{+} monocytes/macrophages (green) in skin DLNs of LPS-treated mice (**C**) when compared to controls (**D**). Infiltrated macrophages in DLNs of LPS (**E**) and PBS (**F**) treated mice were quantified by FACS analysis, and the increase in MOMA-2^{+} cells in skin DLN of LPS injected CD18^{hypo} mice compared to PBS injected CD18^{hypo} mice was found to be statistically significant. p <0.01 (**G**). Cryo-sections derived from injected skin areas of healthy CD18^{hypo} mice at two or 24 hours after LPS injection and lesional skin of affected CD18^{hypo} mice were stained with anti-mouse TNF-α mAb (red). TNF-α was transiently detectable in the dermis two hours after LPS treatment (**H**), but no longer after 24 hours (**I**). As expected, strong TNF-α ex-pression was detected in lesional skin of affected CD18^{hypo} mice (**J**), while in healthy skin of CD18^{hypo} mice no TNF-α was observed (**K**). One representative experiment out of ≥ 3 is shown. (A, B, H - N original magnification, x20; C, D original magnification, x10). e, epidermis; d, dermis; h, hair follicle. A-D, nuclei were counterstained with propidium iodide (red). H-K, nuclei were counterstained with DAPI (blue). Dotted lines indicate the border between epidermis and dermis.

Figure S5: Neutrophils do not causally contribute to the development of the psoriasiform skin disease in the CD18^{hypo} mouse model. To assess the contribution of neutrophils in the pathogenesis of the psoriasiform inflammatory lesions in the CD18^{hypo} mouse model, neutrophils were depleted by repetitive administrations of 250 µg neutralizing antibody anti-mouse GR-1 into severely affected CD18^{hypo} PL/J mice. The clinical picture of a

representative mouse (n = 3) prior to (**A**) and 42 days after treatment (**B**). Clinical assessment of the disease severity using the adapted PASI score shows that a slight increase in disease severity occurred after depletion of neutrophils most likely reflecting the natural course of the disease (**C**). GR-1^+ neutrophil depletion was confirmed by immunofluorescence staining of skin samples and FACS analysis of peripheral blood cells. Cryosections from skin samples of lesional skin before (**D**) and at day 42 of treatment with neutrophil depleting antibodies (**E**) stained with the neutrophil specific marker GR-1-PE (red). Depletion of GR-1^+ neutrophils was fully achieved during the treatment. Cell nuclei were counterstained with DAPI (blue) (original magnification, x20). e, epidermis; d, dermis; h, hair follicle. Dotted lines indicate the border between epidermis and dermis. FACS analysis of whole peripheral blood confirmed the efficient depletion of GR-1 positive cells (**F**).